- Technical Paper -

SHEAR STRENGTH OF REINFORCED CONCRETE MEMBERS STRENGTHENED WITH FRP JACKETING

Tidarut JIRAWATTANASOMKUL[*1], Yoshifumi IKOMA[*2], Dawei ZHANG [*3] and Tamon UEDA[*4]

ABSTRACT

The objective of this study is to propose a new model to predict the ultimate shear strength of RC members with and without FRP jacketing. This paper shows that the proposed model can predict the shear strength in the pre-flexural yielding range. The proposed model considers the confinement effect and the stiffness of reinforcement on the shear strength. The enhancement of shear strength by the confinement effect of FRP jacketing and the application of jacketing with a high fracture strain fiber can be predicted by the model. The proposed model shows a good agreement with the testing results.

Keywords: shear strength, reinforcement stiffness, confinement, FRP jacketing, PET fiber

1. INTRODUCTION

Insufficiency of shear strength and ductility of existing structures is one of the major causes of the brittle shear failure observed in Reinforced Concrete (RC) structures. Consequently, improvement of shear strength and ductility in such structures is necessary to ensure the safety of structures. Worldwide attention has emphasized more on shear strengthening of those deficient structures by Fiber-Reinforced Polymers (FRP). This is due to the various advantages of FRP such as high corrosion resistance and better long-term durability. Conventional strengthening materials such as steel always suffer from the corrosion problem which increases life cycle cost. However, the brittleness of FRP has been a major obstacle and reduces the ductility of the structure especially under seismic effects. To overcome the early breakage of the fiber and increase ductility, the use of a new type of fiber with high fracturing strain, PET (Polyethylene Terephthalate) has been developed [1,2].

Currently the shear strength models regarding to the design for strengthening with FRP are implemented in JSCE code [3]. However, the confinement effect from the FRP-jacketing has not been considered in the shear strength model in the code. In reality, the influence of confinement effect to the shear behavior of FRP-jacketed members should be clarified through theoretical as well as experimental studies in order to predict the precise shear behavior. Moreover, most of the existing members have suffered from the damages prior to the FRP-strengthening. Therefore, it is necessary to investigate the effect of the damage level on the shear strength simultaneously.

In order to predict the shear strength of RC members with and without FRP jacketing, the authors proposed a new model which emphasizes on the confinement effect on the shear strength model. Another main focus is to investigate the pre-damage level on the shear strength components which are concrete and shear reinforcement resisting forces. This paper presents the applicability of the proposed model which is verified and compared with the experimental results of RC members with and without FRP jacketing.

2. PROPOSED SHEAR STRENGTH MODEL

2.1 SHEAR STRENGTH MODEL

The previous experimental evidences [1,2,4] showed that shear strength of members significantly relates to the effective stiffness of tension or shear reinforcement and compressive strength of concrete (f'_c). General concepts of the strength model and failure modes are illustrated in Fig. 1. When the flexural reinforcement reaches its yielding stress (V_y), the reduction of flexural stiffness occurs and then the potential shear strength (V_{su}) drops. The potential shear capacity decreases further after yielding of shear reinforcement. This is because the contribution of concrete on the potential shear capacity decreases further with reduction of aggregate interlocking and concrete compression zone whereas the shear reinforcement contribution has no further increase.

Considering the failure modes existing in a member (see Fig. 1), the load carrying capacity starts to decrease when the potential shear strength curve intersects with the flexural strength curve (mode I, II and III). Brittle shear failure in the pre-flexural yielding range takes place when the potential shear strength intersects the flexural strength before the flexural yielding is reached (mode I). In the post-yielding region, both mode III and IV fail after the development of

*1 Graduate student, Graduate School of Engineering, Hokkaido University, M.E, JCI Member
*2 Undergraduate student, School of Engineering, Hokkaido University
*3 Post-doctoral fellow, Faculty of Engineering, Hokkaido University, PhD. JCI Member
*4 Prof., Faculty of Engineering, Hokkaido University, Dr.E., JCI Member

maximum flexural strength (V_{mu}) so the ductile behavior is achieved. In case of the flexural failure, there is no intersection of two strength curves, meaning no effect of the shear failure (mode IV).

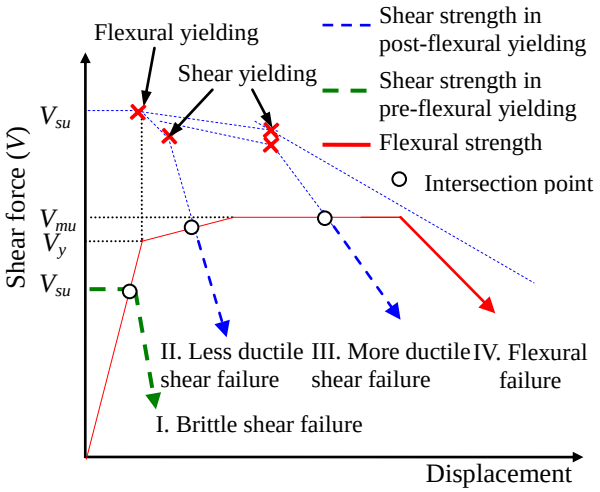

Fig.1 Failure modes in pre- flexural yielding and post-flexural yielding

2.2 SHEAR STRENGTH COMPONENTS

To estimate the size of concrete compression zone, the shear strength equations of cut plane (section A-A as in Fig. 2) are developed [4]. The neutral axis depth, affected by various factors, becomes smaller in shear cracking zone (x_e) than that by the bending theory (x). Thus, the depth of compression zone is expressed as follows:

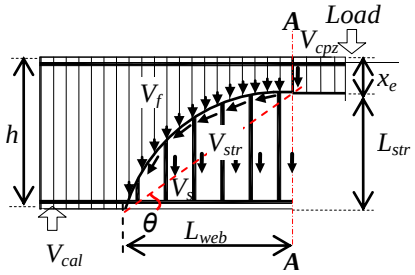

V_c = concrete resisting shear force $=V_{cpz}+V_{str}$
V_{cpz} = compressive concrete resisting force
V_{str} = aggregate interlocking resisting force
V_{web} = transverse reinforcement resisting force
$=V_s+V_f$

Fig.2 Shear strength mechanism

$$\frac{x_e}{x}=\left[\frac{1-e^{-0.42\frac{a}{d}}}{1+3.2^{-0.12\left(\rho_w E_w+\rho_f E_f\right)^{0.4}}}\right]\left[1.25e^{-0.08\left(\frac{\rho_s E_s}{1000}\right)}\right] \quad (1)$$

where: x is the neutral axis depth calculated by bending theory as follows:

$$x=d\left(-n\rho_s+\sqrt{\left(n\rho_s\right)^2+2n\rho_s}\right) \quad (2)$$

where: ρ_s, ρ_w and ρ_f denote the ratio of tension, steel tie and fiber reinforcement respectively. The value of ρ_f and ρ_w can be calculated by $2t_f/b$ and $2A_w/sd$.

The vertical and horizontal projected lengths of the shear cracking region are L_{str} and L_{web} as shown in Fig.2, respectively. However, the angle of the diagonal shear crack (θ) is assumed as 45˚ according to [4], which is a convention assumption. Thus, the actual angle is used to obtain the precise length of shear crack.

$$L_{str}=h-x_e \quad (3)$$

$$L_{web}=\frac{L_{str}}{\tan\theta} \quad (4)$$

According to Sato et al. [4], the concrete shear strength depends on the formation of shear cracking as illustrated in Fig.2. In this study, both the steel tie and fiber are assumed to resist the shear force monolithically and the model to predict this becomes a single term, V_{web}. Thus, total shear strength (V_{cal}) can be calculated as the following equation:

$$V_{cal}=V_c+V_{web} \quad (5)$$

$$V_{web}=bL_{web}\overline{\varepsilon_w}\left(\rho_w E_w+\rho_f E_f\right) \quad (6)$$

From the analysis of the experimental data, it was found that average tensile strain of transverse reinforcement is affected by the same parameters proposed by Sato in his equation [4]. Utilizing a multiple non-linear regression analysis, an empirical formula is proposed to express the average strain of the transverse reinforcement ($\overline{\varepsilon_w}$) where it is considered that fiber strain and steel tie strain have the same value.

$$\overline{\varepsilon_w}=0.004\frac{\sqrt{f'_c}}{\sqrt{\frac{a}{d}}+1}\left(e^{\frac{150}{\rho_s E_s}-0.12\sqrt{\rho_w E_w+\rho_f E_f}}\right) \quad (7)$$

2.3 CONFINEMENT EFFECT

One important application of FRP-jacketing is the confinement effect due to fiber and steel tie. In fact, the confinement effect exists only in the compression region which can be indicated by the neutral axis depth (x_e) and the lateral confining pressure provided by FRP jacket can be calculated by the simplified assumption [5] as in Fig. 3(a).

For simplicity, the effective lateral confining pressure in y-direction ($f_{ly,f}$) is a ratio of the neutral axis depth to the total depth (x_e/h), whereas the lateral confining pressure in x-direction ($f_{lx,f}$) is a half of the total concrete expansion. Therefore, the effective confinement in both directions is expressed in Eq. 8 and Eq. 9.

$$f_{lx,f}=\frac{1}{2}\rho_f\varepsilon_f E_f \quad (8)$$

$$f_{ly,f}=\frac{x_e}{h}\rho_f\varepsilon_f E_f \quad (9)$$

In Fig.3(b), the effective core concrete enclosed by steel tie is proposed as the arching action by Mander et al [6]. In the assumption, the lateral pressure provided by steel tie in x- ($f_{lx,w}$)and y-directions ($f_{ly,w}$) is a function of stiffness of steel tie (E_w) and the strain of steel tie (ε_w) measured from the experiment.

$$f_{lx,w} = k_w \rho_w \varepsilon_w E_w \quad (10)$$

$$f_{ly,w} = k_w \rho_w \varepsilon_w E_w \quad (11)$$

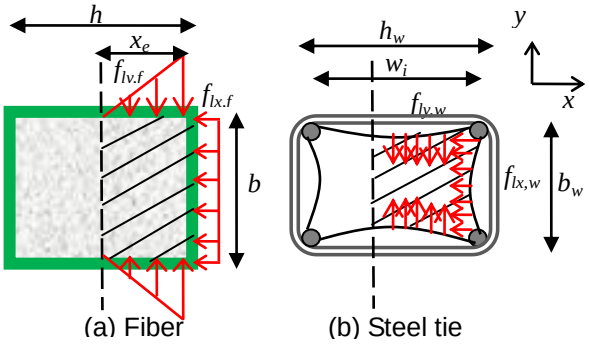

Fig. 3 Lateral confining pressure

Moreover, Mander et al [6] developed the effective confinement coefficient (k_w) as in Eq. 12. The core dimensions to centerlines of perimeter steel tie in x- and y- directions are h_w and b_w, respectively. The clear distance between adjacent longitudinal bars is w_i and s' is a clear vertical spacing of tie reinforcement.

$$k_w = \frac{\left(1 - \sum_{i=1}^{n} \frac{(w_i)^2}{6 b_w h_w}\right)\left(1 - 0.5\frac{s'}{2b}\right)\left(1 - 0.5\frac{s'}{2h}\right)}{(1 - \rho_{cc})} \quad (12)$$

where: A_{cc} = area of the core section enclosed by the center lines of steel tie and ρ_{cc} = ratio of total area of longitudinal reinforcement to area of the core section (A_c).

Since both steel tie and fiber jackets enclose the core section, the total lateral pressure in x- (f_{lx}) and y-directions (f_{lx}) derives from the summation of the lateral pressure provided by fiber sheet and steel tie.

$$f_{lx} = f_{lx,w} + f_{lx,f} \quad (13)$$

$$f_{ly} = f_{ly,w} + f_{ly,f} \quad (14)$$

The maximum lateral stress (f_l) is considered by using the larger value between Eq. 13 and Eq. 14. To address the confinement effect to the concrete strength, Mander et al. [6] proposed the confined compressive strength of concrete (f'_{cc}) as a function of the maximum lateral stress and the unconfined compressive strength (f'_c) as in Eq. 15. In this equation, the concrete strength is equal to the unconfined concrete strength in case of no lateral pressure (f_l=0).

$$f'_{cc} = f'_c\left(-1.254 + 2.254\sqrt{1 + \frac{7.94 f_l}{f'_c}} - 2\frac{f_l}{f'_c}\right) \quad (15)$$

By a non-linear regression approach, the concrete shear strength can be clarified depending on three parameters, stiffness of tension reinforcement ($\rho_s E_s$), shear reinforcement ($\rho_w E_w + \rho_f E_f$) and the concrete strength with confinement (f'_{cc}). To obtain the precise ultimate shear strength, the concrete shear strength model is derived from the best fitting of the measured shear force at the ultimate load as follows:

$$V_c = 5 \cdot b \cdot d \cdot \sqrt[3]{f'_{cc}} \cdot \left\{0.12 \ln\left(\rho_w E_w + \rho_f E_f\right) - 0.12\right\} \times \left\{0.25 \ln\left(\rho_w E_w + \rho_f E_f\right) - 0.25\right\} \cdot \left(\frac{a}{d}\right)^{-1/4} \quad (16)$$

3. EXPERIMENTAL PROGRAMS

3.1 SPECIMEN DETAILS AND INSTRUMENTATION

To verify the reliability of the proposed model in the section 2.3 for the effect of FRP confinement, five RC beams with and without FRP-jacketing identified as B1-B5 were conducted under a monotonic three-point bending load. Since the concrete is mixed in the same batch, the compressive strength of concrete showed an insignificant difference in each specimen. As a result, the authors used the average cylinder compressive strength of concrete as f'_c in Table 1. The details of specimens tested by the authors are summarized in Table 1.

Table 1 Details of specimens

Specimen	f'_c (MPa)	b (mm)	h (mm)	d (mm)	a/d	*Fiber*	p_{sc} *1 (%)	p_s *2 (%)	p_w *3 (%)	p_f *4 (%)	s *5 (mm)	*Pre-loading level*	*Failure mode*
B1	36.0	200	250	212	2.8	None	0.33	2.40	0.11	0.00	150	Failed	S
B2	36.0	200	250	212	2.8	PET	0.33	2.40	0.11	0.84	150	-	F/DB
B3	36.0	200	250	212	2.8	PET	0.33	2.40	0.11	0.84	150	SC	F/DB
B4	36.0	200	250	212	2.8	PET	0.33	2.40	0.11	0.84	150	SC/SY	F/DB
B5	36.0	200	250	212	2.8	PET	0.33	2.40	0.11	0.84	150	SC/SY	F/DB

*1 compression steel ratio, *2 tension reinforcement ratio, *3 steel tie ratio, *4 fiber ratio, *5 spacing of steel tie
S= Shear failure without flexural yielding, F/DB = Flexural failure with debonding of fiber sheet
SC = Diagonal shear crack, SY = Yielding of shear reinforcement

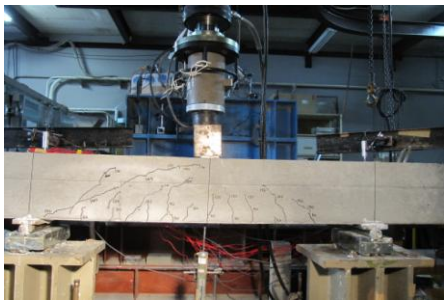

Fig.4 Instrumentation of the control specimen

In Fig. 4, the control specimen, B1, was loaded until it failed in shear with the diagonal shear crack reaching the loading point and the ultimate load is 89.9 kN. To simulate the actual damage of an RC member during its service life, three beams (B3-B5) were preloaded before strengthening by FRP whereas the beam, B2, is strengthened without the pre-damage. The level of the preloading is separated into three stages based on the influences of shear crack, yielding of shear reinforcement and ultimate load. From the experimental observation, the FRP-jacketed specimens showed the enhancement of shear capacity and the failure mode shifted to be flexural failure.

force carried by concrete as shown in Fig. 6. Furthermore, the specimen without the pre-damage (B2) shows higher concrete shear force than that of damaged specimens. It is proved that the shear strength of concrete decreased due to the pre-damage.

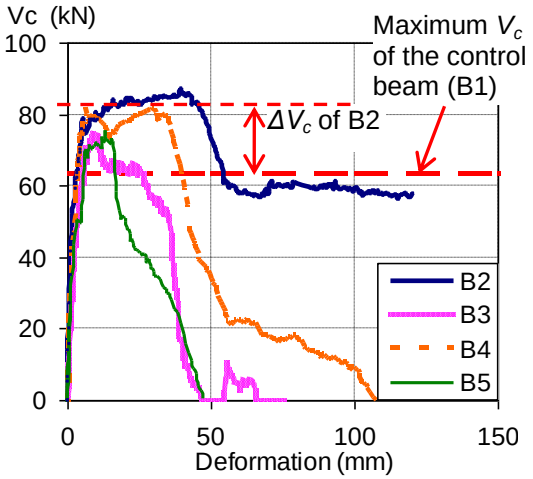

Fig.6 Shear force carried by concrete

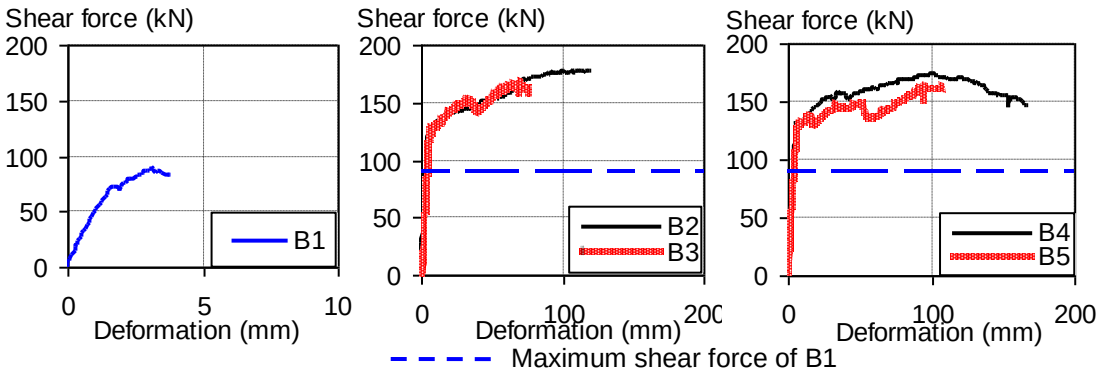

Fig.5 Shear force and deformation of B1-B5

The relations between applied shear force and central deflection of each specimen are shown in Fig.5. At ultimate load, the total shear force of the pre-damaged beams (B3-B5) is insignificantly different from that of the non-damaged beam (B2). It can be implied that the pre-damage does not affect the total shear force because the shear force provided by fiber sheet compensates the reduction of the shear force due to the pre-damage.

3.2 INFLUENCE OF THE CONFINEMENT

The shear force carried by concrete can be obtained by subtracting the total shear force by the shear force carried by steel tie and fiber (V_{exp}-V_s-V_f). Here, the shear force contributed by both steel tie and fiber is taken corresponding to the measured strain gauge. Considering the increment of the maximum shear force carried by concrete (e.g. ΔV_c of B2 in Fig. 6), the value of V_c from the unretrofitted members (B1) is compared with the V_c-value observed from retrofitted members. Therefore, retrofitting of the damaged specimens with FRP results in an increase of the shear

Fig. 7 shows the comparison between the concrete compressive strength with PET-fiber jacketing confinement obtained from Eq. 15 and the ΔV_c normalized by the V_c of the control beam without confinement. The confined concrete has an enhancement of the shear strength around 10-50%, which clearly indicates the effect of PET-fiber confinement.

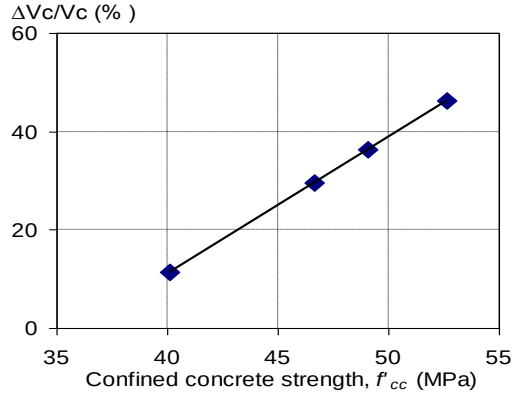

Fig. 7 Influence of f'_{cc} to $\Delta V_c/V_c$

Table 2 Summary of analytical parameters and experimental results

Specimen	f'_c (MPa)	f'_{cc} (MPa)	a/d	p_sE_s	$p_w E_w$	$p_f E_f$	$V_{c\text{-}cal}$ (kN)	$V_{s\text{-}cal}$ (kN)	V_{exp} (kN)	V_{cal} (kN)	V_{exp}/V_{cal} (kN)
B1	36.0	36.0	2.8	209.0	188.1	0.00	83.3	42.2	90.0	125.4	0.72
B2	36.0	52.7	2.8	209.0	188.1	0.00	106.4	72.7	*N/A*	179.1	*N/A*
B3	36.0	46.6	2.8	209.0	188.1	0.00	101.7	66.3	*N/A*	168.0	*N/A*
B4	36.0	49.1	2.8	209.0	188.1	0.00	103.7	69.0	*N/A*	172.6	*N/A*
B5	36.0	40.1	2.8	209.0	188.1	0.00	95.6	58.7	*N/A*	154.3	*N/A*
SP1[2)]	25.3	25.3	2.5	336.6	290.7	0.00	136.1	58.4	178.4	194.6	0.92
SP2[2)]	25.3	35.5	2.5	336.6	290.7	12.1	149.4	70.7	232.3	220.2	1.06
SP3[2)]	25.3	31.0	2.5	336.6	290.7	18.7	145.1	66.8	229.3	211.9	1.08
SP4[2)]	25.3	39.8	2.5	336.6	290.7	24.2	155.1	76.4	259.8	231.6	1.12
SP5[2)]	25.3	34.1	2.5	336.6	290.7	37.4	150.5	72.2	248.4	222.8	1.11
R8[7)]	26.7	26.7	3.36	286.9	289.8	0.00	75.7	30.2	81.2	105.9	0.77
R9[7)]	29.6	29.6	3.36	860.7	869.4	0.00	117.0	20.7	106.4	137.7	0.77
R10[7)]	29.6	29.6	3.36	430.4	434.7	0.00	91.2	31.9	76.7	123.2	0.62
R11[7)]	26.0	26.0	3.36	430.4	434.7	0.00	94.7	25.9	91.2	120.6	0.76
R12[7)]	34.0	34.0	3.6	860.7	869.4	0.00	126.9	16.7	111.6	143.6	0.78
R13[7)]	32.3	32.3	3.6	286.9	289.8	0.00	77.6	26.9	152.4	104.5	1.46
R14[7)]	29.0	29.0	3.36	860.7	869.4	0.00	116.4	20.5	91.2	136.9	0.67
R15[7)]	29.9	29.9	3.6	430.4	434.7	0.00	89.4	24.0	142.4	113.4	1.26
R16[7)]	31.6	31.6	3.6	430.4	434.7	0.00	97.2	23.7	142.4	120.9	1.18
R20[7)]	43.0	43.0	3.36	286.9	289.8	0.00	85.2	38.3	91.6	123.6	0.74
R21[7)]	48.2	48.2	3.6	860.7	869.4	0.00	129.2	20.8	152.4	150.0	1.02
R22[7)]	29.5	29.5	4.5	430.4	434.7	0.00	82.7	26.0	81.2	108.7	0.75
R23[7)]	30.2	30.2	2.24	430.4	434.7	0.00	112.5	35.5	100.7	148.1	0.68
R24[7)]	30.9	30.9	5.05	860.7	869.4	0.00	110.7	13.0	93.9	123.7	0.76
R25[7)]	30.8	30.8	3.6	860.7	869.4	0.00	115.5	16.6	106.6	132.1	0.81
R26[7)]	36.6	36.6	2.4	430.4	434.7	0.00	107.6	33.2	152.4	140.8	1.08
R27[7)]	13.7	13.7	3.6	430.4	434.7	0.00	78.8	15.6	96.6	94.5	1.02
R28[7)]	31.6	31.6	3.6	860.7	857.8	0.00	124.3	16.3	182.8	140.6	1.30

N/A = cannot observe the ultimate load due to the flexural failure

4. VERIFICATION OF SHEAR STRENGTH MODELS

The experimental results of PET shear-strengthened RC members which failed in shear [2,7] were taken to verify the applicability of the proposed shear strength model in pre-flexural yielding range, which means the shear failure occurred before the yielding of tension reinforcement in all referred specimens. In Table 2, the analytical parameters are taken to estimate the shear. The analytical parameter consists of the compressive strength of concrete (f'_c) which is from the experimental observation whereas the confined compressive strength (f'_{cc}) is from Eq. 15. The other parameters are shear span to the depth ratio (a/d), the stiffness of tension reinforcement (p_sE_s), steel tie (p_wE_w) and fiber (p_fE_f). In this study, the shear strength components consist of shear strength contributed by concrete (V_c) and shear reinforcement (V_s) so the verification of shear strength can separate in each component, if the data is available. The experimental and calculation results are presented in Table 2.

4.1 VERIFICATION OF SHEAR STRENGTH COMPONENTS

In this section, the experimental results tested by the authors are shown as a blue rectangular marker in all the graphs. Starting from the comparison between calculated and experimental concrete shear strength, the results from the experiment and model are illustrated in Fig. 8. The concrete shear strength is considered from the actual shear contribution of concrete at ultimate load. However, the experimental observations showed the reduction of concrete shear strength after the shear crack becomes wider which leads to not only the loss of shear force due to the aggregate inter-locking and also the decrease of concrete compression zone. The proposed model shows a good correlation with the experimental results in terms of concrete shear strength.

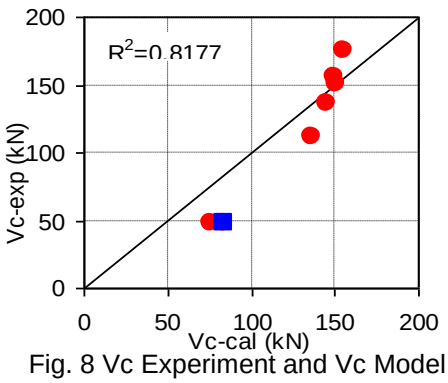

Fig. 8 Vc Experiment and Vc Model

In Fig. 9, the shear strength carried by fiber and steel tie obtained from the model is conservative compared with the experimental results. This is because the shear crack is assumed to be equal to 45˚. With this assumption, the number of fiber and steel tie across the shear crack is slightly underestimated. In fact, the inclination of the shear crack is smaller than the assumed value so the calculated shear force shows conservative value.

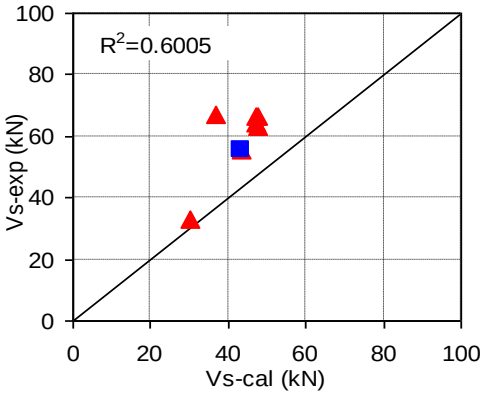

Fig. 9 Vs Experiment and Vs Model

4.2 VERIFICATION OF ULTIMATE SHEAR STRENGTH

The ultimate shear strength from the experiment [2,7] is compared with the total shear strength (V_{cal} $=V_c+V_s$) predicted by the proposed model. In Fig.10, the V_{cal} correlates well with the shear strength observed in the experiment with and without PET strengthening.

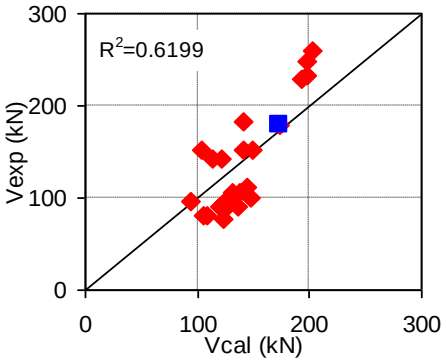

Fig. 10 V_{exp} Experiment and V_{cal} Model

From the verification of the model, the proposed model can be applied to RC members jacketed PET fiber sheet which has high fracturing strain. However, the further study is required to develop the shear strength model for other fiber sheets with low fracturing strain.

5. CONCLUSIONS

This paper presented a new shear strength model taking into account several parameters such as the effect of fiber confinement, stiffness of reinforcement, tension reinforcement ratio, fiber ratio, shear span to depth ratio and concrete strength. Experiments of five RC beams with and without FRP-jacketing were conducted to verify the reliability of proposed model for the FRP confinement effect. Additional experimental databases available in the literatures were collected to verify the applicability and reliability of the proposed model for the shear strength prediction. The conclusion of this study is as follows:

(1) The proposed model can predict the increase of concrete shear strength due to the confinement effect provided by the FRP jacket with high fracturing fiber, such as PET.
(2) The proposed model can predict well the shear strength components carried by shear reinforcement, such as stirrup and FRP jacket.
(3) The proposed model can predict the total shear strength of reinforced concrete beams with and without PET-fiber jacketing in the pre-flexural yielding range. The experimental program is well correlated with the proposed predictive model.
(4) The pre-damage reduces the shear force carried by concrete. However, the total shear force does not decrease because the fiber sheet compensates the reduction of the concrete shear force due to the pre-damage.

ACKNOWLEDGEMENT

The authors would like to acknowledge Maeda Kosen Co.Ltd., Japan for providing the PET sheet.

REFERENCES

[1] Anggawidjaja, D. and Ueda, T.: “PET, High Fracturing Strain Fiber, for Concrete Structure Retrofitting: Shear Force and Deformation Enhancement: Experiments, Analysis and Model,” VDM Verlag Dr. Müller, 2009, pp.1-64.
[2] Senda, M.: Shear Strengthening by FRP Sheet, Graduation Thesis, Hokkaido University, April 2006 (in Japanese).
[3] Japan Society of Civil Engineers (JSCE): “Recommendations for upgrading of concrete structures with use of continuous fiber sheets,” Concrete engineering series 41, pp. 250, 2001
[4] Sato, Y., Ueda, T., and Kakuta, Y.: “Shear Strength of Prestressed Concrete Beams with FRP Tendon,” JSCE, Vol. 28, No.27, pp. 189-208, 1995
[5] Jirawattanasomkul, J., Anggawidjaja, D. and Ueda, T.: “Seismic Retrofitting by FRP Jacketing and Prediction Method of Ultimate Deformation,” CICE - The 5th International Conference on FRP Composites in Civil Engineering, 2010
[6] Mander, JB., Priestley, MJN. and Park, R.: “Theoretical Stress–strain Model for Confined Concrete,” ASCE Journal of Structural Engineering, Vol. 114, No.8, pp. 1804–1826,1988
[7] Placas, A. and Regan, P.E.: Shear Failure of Reinforced Concrete Beams. ACI Journal, Vol.68, No.10, pp. 763-774, 1971